Chin. J. Mech. Eng. (2017) 30:982–990
DOI 10.1007/s10033-017-0143-z

ORIGINAL ARTICLE

Estimation of Road Friction Coefficient in Different Road Conditions Based on Vehicle Braking Dynamics

You-Qun Zhao[1] · Hai-Qing Li[1] · Fen Lin[1] · Jian Wang[2] · Xue-Wu Ji[3]

Received: 12 October 2015 / Revised: 13 April 2017 / Accepted: 20 April 2017 / Published online: 3 May 2017

Abstract The accurate estimation of road friction coefficient in the active safety control system has become increasingly prominent. Most previous studies on road friction estimation have only used vehicle longitudinal or lateral dynamics and often ignored the load transfer, which tends to cause inaccurate of the actual road friction coefficient. A novel method considering load transfer of front and rear axles is proposed to estimate road friction coefficient based on braking dynamic model of two-wheeled vehicle. Sliding mode control technique is used to build the ideal braking torque controller, which control target is to control the actual wheel slip ratio of front and rear wheels tracking the ideal wheel slip ratio. In order to eliminate the chattering problem of the sliding mode controller, integral switching surface is used to design the sliding mode surface. A second order linear extended state observer is designed to observe road friction coefficient based on wheel speed and braking torque of front and rear wheels. The proposed road friction coefficient estimation schemes are evaluated by simulation in ADAMS/Car. The results show that the estimated values can well agree with the actual values in different road conditions. The observer can estimate road friction coefficient exactly in real-time and resist external disturbance. The proposed research provides a novel method to estimate road friction coefficient with strong robustness and more accurate.

Keywords Road friction coefficient · Real time estimation · External disturbance · Different road conditions

1 Introduction

It is a powerful means to improve vehicle driving safety and stability performances via active safety system such as emergency collision avoidance (ECA), active front steering (AFS), anti-lock braking system (ABS), direct yaw moment control (DYC) and traction control system (TCS) [1–6]. They work well only with the tire forces within the friction limit, which means knowledge of the road friction coefficient may improve the performance of the systems. For example, during a steering process, the lateral tire force is limited by the road friction coefficient. The vehicle would drift out if the vehicle steers severely at a relatively high speed because of limitation of the lateral tire force. If the active control system could estimate the friction limitation at the time driver begins to steer and initiatives to reduce the speed, the lateral dynamics of the vehicle would be improved [4]. Wheel braking under the different road condition, we usually can't get the real-time value of road friction coefficient, which leads the instability of the whole control process [7, 8]. So road friction coefficient has an important significance in the vehicle chassis electronic control system design. The accurate estimation of the road friction coefficient can facilitate the improvement of the active safety system and attain a better performance in operating vehicle safety systems. Active safety system can

Supported by Fundamental Research Funds for the Central Universities (Grant No. NS2015015).

✉ Fen Lin
flin_nuaa@163.com

[1] College of Energy & Power Engineering, Nanjing University of Aeronautics and Astronautics, Nanjing 210016, China

[2] School of Automotive Engineering, Shandong Jiaotong University, Jinan 250023, China

[3] State Key Laboratory of Automotive Safety and Energy, Tsinghua University, Beijing 100084, China

automatically adjust the control strategy according to changing of road surfaces with respect to the friction properties, and which can maximize the function of the control system.

In recent years, to obtain road friction coefficient, many scholars have proposed various estimation methods [8–21]. Among them, domestic scholars especially Liang LI and their teams used signal fusion method [8, 9], double cubature kalman filter method [10], and observer [11] to estimate the road friction coefficient. Generally speaking, they are mainly classified into two groups of special-sensor-based [12–14] methods and vehicle-dynamics-based methods, also known as Cause-based and Effect-based [15]. Method of Cause-based was used by optical sensors to measure light absorption and scattering of road according to the road surface shapes and physical properties. This method looks simple and direct, but has practical issue of cost, which limits its use in production vehicle. Effect-based method was presented by measuring the related response of vehicle dynamics model and applies extended kalman filtering or other algorithm to obtain its value. The vehicle dynamics model included both longitudinal and/or lateral dynamics [16, 17]. The main features of these methods could make full use of the on-board sensors and reduce costs, which has been widely used.

Two very similar studies [18, 19] used the kalman filter (KF) to estimate the longitudinal force of the vehicle first and then through the recursive least squares (RLS) method and the change of CUSUM estimated the road friction coefficient. Wenzel, et al. [20], reported another method of the dual extended kalman filter (DEKF) for road friction coefficient estimation. Comparing kalman filter algorithm and the extended kalman filtering algorithm, Ref. [21] design a extended state observer (ESO) by means of the dynamics model of 1/4 tire for braking to estimate road friction coefficient. This method can ensure high calculation accuracy and do not need to solve Jacobian trial.

This article, considering load transfer of front and rear axles, the braking dynamic model of two-wheeled vehicle was built. Sliding mode control method was used to build the ideal braking torque controller, which control objective is to control the actual wheel slip ratio of front and rear wheels tracking the ideal wheel slip ratio. In order to eliminate chattering problem of the sliding mode controller, integral switching surface was used to design the sliding mode surface. Road friction coefficient can be observed by second order linear extended state based on wheel speed and braking torque of front and rear wheels. Comparing with the article discussed, this method considered the effect of axle load transfer to the road friction coefficient estimation. It has both fewer parameters taking into account and higher computational efficiency.

2 Vehicle Braking Dynamics Model

2.1 Full-Vehicle Model

The assumptions for the vehicle model are as follows: (1) Neglect the effect of road slope; (2) Ignore the load transfers by the lateral accelerations; (3) The effects of air resistance and rolling resistance of tire are neglected; (4) Ignore the effects of transmission system, steering system and suspension system on vehicle. Vehicle model presented here is a two-wheeled vehicle model with the sketch given in Fig. 1.

From Fig. 1, the body motions of longitudinal and yaw can be described, respectively, by Eqs. (1)–(4) as follows:

$$\dot{x} = V, \tag{1}$$

$$\dot{V} = -g\frac{\mu(\lambda_f)m_1 + \mu(\lambda_r)m_2}{m - \mu(\lambda_f)m_3 + \mu(\lambda_r)m_3}, \tag{2}$$

$$\dot{\omega}_f = \frac{1}{2J_f}(-T_{bf} + \mu(\lambda_f)m_1R_\omega g - \mu(\lambda_f)m_3R_\omega\ddot{x}), \tag{3}$$

$$\dot{\omega}_r = \frac{1}{2J_r}(-T_{br} + \mu(\lambda_r)m_2R_\omega g + \mu(\lambda_r)m_3R_\omega\ddot{x}), \tag{4}$$

where

$$m_1 = \frac{l_r}{l_f + l_r}m\ ,\ m_2 = \frac{l_f}{l_f + l_r}m\ ,\ m_3 = \frac{m_f h_f + m_s h_s + m_r h_r}{l_f + l_r},$$

where $\mu(\lambda_f)$ and $\mu(\lambda_r)$ are the road friction coefficient of front and rear wheels,m is the total mass of vehicle, V is the vehicle longitudinal velocity, T_{bf} and T_{br} are the braking torque of front and rear wheels, J_f and J_r are the moment of inertia of front and rear wheels, ω_f and ω_r are the angular speed of front and rear wheels, R_ω is the wheel rolling radius.

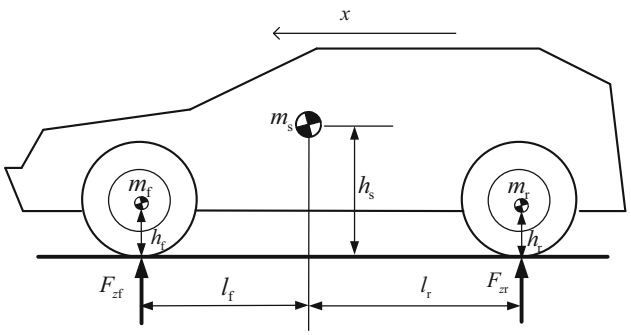

Fig. 1 Two-wheeled vehicle model. h_f, h_r—Height of vehicle front, rear unsprung mass, l_f, $l_r\psi$—Distance between centre of gravity and the front, rear axes, F_{zf}, F_{zr}—Vertical forces of vehicle front, rear tire, m_f,m_r—Front, rear unsprung mass, x—Displacement in the process, m_s—Sprung mass of vehicle, h_s—Height of vehicle sprung mass

2.2 Full-Vehicle Model

Tire force is so important that it influences the precision of simulation. The tire model should reflect the effect of tire vertical force on longitudinal and lateral forces, and the interaction of longitudinal and lateral forces. In order to predict the vehicle longitudinal force in braking conditions, Burckhardt model is introduced by theoretical deformation and simulation analyses on the basis of the Magic Formula model [22, 23]. It provides the tire-road coefficient of friction μ as a function of the wheel slip λ and the vehicle velocity V. The equation can be described as

$$\mu(\lambda, V) = (C_1(1 - \exp(C_2\lambda)) - C_3\lambda)\exp(-C_4\lambda V), \quad (5)$$

where C_1, C_2 and C_3 are the characteristic parameters of tire adhesion; C_4 is the influence parameter of car speed to adhesion and is in the range 0.02–0.04. Table 1 shows friction model parameters for different road conditions.

Fig. 2 illustrates the relationship of road friction coefficient vs. slip ratio at different road conditions.

As can be seen from the figure, Burckhardt tire model describes the nonlinear change law of road friction coefficient vs. wheel slip rate is good.

3 Braking Torque Controller Design

3.1 Braking Torque Design

The front and rear wheel longitudinal slip ratio can be described as.

$$\lambda_f = \frac{V - \omega_f R_\omega}{V}, \quad (6)$$

$$\lambda_r = \frac{V - \omega_r R_\omega}{V}, \quad (7)$$

where λ_f and λ_r denotes the front and rear wheel longitudinal slip ratio respectively and the derivative of which with respect to time are, respectively, given by.

$$\dot{\lambda}_f = \frac{\dot{V}(1 - \lambda_f) - \dot{\omega}_f R_\omega}{V}, \quad (8)$$

Table 1 Friction model parameters of different road

Road surface conditions	C_1	C_2	C_3
Dry asphalt	1.2801	23.990	0.5200
Dry concrete	1.1973	25.186	0.5373
Snow	0.1946	94.129	0.0646
Ice	0.0500	306.390	0.0000

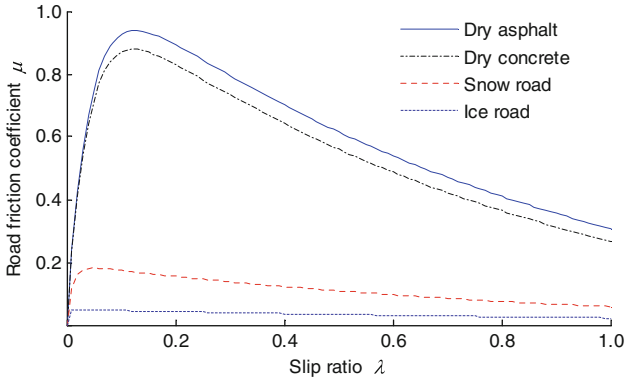

Fig. 2 Relationship of road friction coefficient vs. slip ratio

$$\dot{\lambda}_r = \frac{\dot{V}(1 - \lambda_r) - \dot{\omega}_r R_\omega}{V}. \quad (9)$$

Substituting Eqs. (8), (9) into vehicle dynamics equation, then

$$\dot{V} = f_2(\lambda_f, \lambda_r), \quad (10)$$

$$\dot{\lambda}_f = \frac{f_2(\lambda_f, \lambda_r)(1 - \lambda_f) - R_\omega f_3(\lambda_f, \lambda_r) + u_f}{V}, \quad (11)$$

$$\dot{\lambda}_r = \frac{f_2(\lambda_f, \lambda_r)(1 - \lambda_r) - R_\omega f_4(\lambda_f, \lambda_r) + u_r}{V}, \quad (12)$$

where

$$f_2(\lambda_f, \lambda_r) = -g\frac{\mu(\lambda_f)m_1 + \mu(\lambda_r)m_2}{m - \mu(\lambda_f)m_3 + \mu(\lambda_r)m_3},$$

$$f_3(\lambda_f, \lambda_r) = \frac{1}{2J_f}(\mu(\lambda_f)m_1 R_\omega g - \mu(\lambda_f)m_3 R_\omega f_2),$$

$$f_4(\lambda_f, \lambda_r) = \frac{1}{2J_r}(\mu(\lambda_r)m_2 R_\omega g + \mu(\lambda_r)m_3 R_\omega f_2),$$

$$u_f = \frac{T_{bf} R_\omega}{2J_f}, \quad u_r = \frac{T_{br} R_\omega}{2J_r}.$$

It can be assumed that the front and rear wheel friction coefficient change between 0 and 1 and vehicle total mass changes within a certain range, namely

$$m_1^- \le m_1 \le m_1^+, \quad (13)$$

$$m_2^- \le m_2 \le m_2^+, \quad (14)$$

$$m_3^- \le m_3 \le m_3^+, \quad (15)$$

$$m^- \le m \le m^+, \quad (16)$$

$$0 \le \mu(\lambda_f), \quad \mu(\lambda_r) \le 1, \quad (17)$$

where the variation range of f_2, f_3 and f_4 can be, respectively, expressed as

$$-g \le f_2(\lambda_f, \lambda_r) \le 0, \quad (18)$$

$$0 \le f_3(\lambda_f, \lambda_r) \le \frac{R_\omega g}{2J_f}(m_1^+ + m_3^+), \tag{19}$$

$$\min\left[\frac{R_\omega g}{2J_r}(m_2^- - m_3^+), 0\right] \le f_4 \le \frac{R_\omega g}{2J_r} m_2^+. \tag{20}$$

The approximate values of f_2, f_3 and f_4 are expressed as

$$\hat{f}_2(\lambda_f, \lambda_r) = -0.5g, \tag{21}$$

$$\hat{f}_3(\lambda_f, \lambda_r) = \frac{R_\omega g}{4J_f}(m_1^+ + m_3^+), \tag{22}$$

$$\hat{f}_4(\lambda_f, \lambda_r) = \frac{1}{2}\left\{\min\left[\frac{R_\omega g}{2J_r}(m_2^- - m_3^+), 0\right] + \frac{R_\omega g}{2J_r} m_2^+\right\}. \tag{23}$$

Define $|f_2 - \hat{f}_2| \le F_2$, $|f_3 - \hat{f}_3| \le F_3$, and $|f_4 - \hat{f}_4| \le F_4$, Eqs. (21), (22) and (23) can be converted into the following forms:

$$F_2 = 0.5g, \tag{24}$$

$$F_3 = \frac{R_\omega g}{4J_f}(m_1^+ + m_3^+), \tag{25}$$

$$F_4 = \frac{R_\omega g}{2J_r} m_2^+ - \frac{1}{2}\left\{\min\left[\frac{R_\omega g}{2J_r}(m_2^- - m_3^+), 0\right] + \frac{R_\omega g}{2J_r} m_2^+\right\}. \tag{26}$$

Define the difference between the actual and target slip ratio of front and rear wheels as the switching surface of sliding mode. The equations can be described as

$$S_1 = \tilde{\lambda}_f = \lambda_f - \lambda_{fd}, \tag{27}$$

$$S_2 = \tilde{\lambda}_r = \lambda_r - \lambda_{rd}, \tag{28}$$

where λ_f and λ_r denotes the actual slip ratio of front and rear wheels respectively, λ_{fd} and λ_{rd} denotes the target slip ratio of front and rear wheels respectively. To attain the equivalent control torque, the derivative of Eqs. (27), (28) with respect to time are, respectively, given by

$$T_{eq.bf} = \frac{2J_f}{R_\omega}\left[\dot{\lambda}_{fd} V - \hat{f}_2(\lambda_f, \lambda_r)(1 - \lambda_f) + R_\omega \hat{f}_3(\lambda_f, \lambda_r)\right], \tag{29}$$

$$T_{eq.br} = \frac{2J_r}{R_\omega}\left[\dot{\lambda}_{rd} V - \hat{f}_2(\lambda_f, \lambda_r)(1 - \lambda_r) + R_\omega \hat{f}_4(\lambda_f, \lambda_r)\right], \tag{30}$$

The brake torque of front and rear wheels is given as

$$T_b = T_{eq.b} - k\,\mathrm{sgn}(S). \tag{31}$$

By accessibility conditions of switching surface, inequality must to be satisfied as follows:

$$S\dot{S} \le 0. \tag{32}$$

The ideal brake torque of front and rear wheels is defined as

$$T_{bf} = \frac{2J_f}{R_\omega}\left[\begin{array}{l}\dot{\lambda}_{fd} V - \hat{f}_2(\lambda_f, \lambda_r)(1 - \lambda_f) + R_\omega \hat{f}_3(\lambda_f, \lambda_r) \\ -(F_f(\lambda_f, \lambda_r) + \eta_1)\mathrm{sgn}(S_1)\end{array}\right], \tag{33}$$

$$T_{br} = \frac{2J_r}{R_\omega}\left[\begin{array}{l}\dot{\lambda}_{rd} V - \hat{f}_2(\lambda_f, \lambda_r)(1 - \lambda_r) + R_\omega \hat{f}_4(\lambda_f, \lambda_r) \\ -(F_r(\lambda_f, \lambda_r) + \eta_2)\mathrm{sgn}(S_2)\end{array}\right]. \tag{34}$$

Respectively

$$F_f(\lambda_f, \lambda_r) = F_2(1 - \lambda_f) + R_\omega F_3,$$

$$F_r(\lambda_f, \lambda_r) = F_2(1 - \lambda_r) + R_\omega F_4,$$

where η_1, η_2 are positive constants.

3.2 Eliminate chattering

Chattering phenomena is one of the undesirable effects of sliding mode control. In order to eliminate the chattering phenomena in sliding mode control, a saturated function $\mathrm{sat}(S/\varphi)$ was introduced and the sliding mode controller was redesigned using integral switching surface to make the control law smooth [24]. Defining integral switching surface as

$$S_1 = \lambda_f - \lambda_{fd} + \xi_1 \int (\lambda_f - \lambda_{fd})\mathrm{d}t, \tag{35}$$

$$S_2 = \lambda_r - \lambda_{rd} + \xi_2 \int (\lambda_r - \lambda_{rd})\mathrm{d}t, \tag{36}$$

where ξ_1 and ξ_2 are the constant.

Using the method of integral switching surface, the ideal brake torque of front and rear wheels are, respectively, given by

$$T_{bf} = \frac{2J_f}{R_\omega}\left[\begin{array}{l}(\dot{\lambda}_{fd} - \xi_1\tilde{\lambda}_f)V - \hat{f}_2(\lambda_f, \lambda_r)(1 - \lambda_f) + R_\omega \hat{f}_3(\lambda_f, \lambda_r) \\ -(F_f(\lambda_f, \lambda_r) + \eta_1)\mathrm{sat}\left(\dfrac{\tilde{\lambda}_f + \xi_1 \int \tilde{\lambda}_f \mathrm{d}t}{\varphi_1}\right)\end{array}\right], \tag{37}$$

$$T_{br} = \frac{2J_r}{R_\omega}\left[\begin{array}{l}(\dot{\lambda}_{rd} - \xi_2\tilde{\lambda}_r)V - \hat{f}_2(\lambda_f, \lambda_r)(1 - \lambda_r) + R_\omega \hat{f}_4(\lambda_f, \lambda_r) \\ -(F_r(\lambda_f, \lambda_r) + \eta_2)\mathrm{sat}\left(\dfrac{\tilde{\lambda}_r + \xi_2 \int \tilde{\lambda}_r \mathrm{d}t}{\varphi_2}\right)\end{array}\right], \tag{38}$$

where φ_1 and φ_2 are the constant, $\varphi_1$and φ_2 are the boundary layer thickness which is made varying to take

advantage of the system bandwidth. How to get the values are introduced by Ref. [23].

4 Road Friction Coefficient Observer Design

Linear extended state observer can expand the uncertainties and unknown perturbation controlled object model into new state observation and it is very suitable for road friction coefficient estimation problems which only have the measured output and control input [25, 26]. Using the linear extended state observer, road friction coefficient can be observed, where friction coefficient between tire and road as output of the second order linear extended state and angular speed and braking torque of front and rear wheels as the input.

By section 2.1 two-wheeled vehicle braking dynamics model we can obtain

$$\begin{cases} \dot{\omega}_{\mathrm{f}} = \dfrac{1}{2J_{\mathrm{f}}}(-T_{\mathrm{bf}} + \mu(\lambda_{\mathrm{f}})m_1R_{\omega}g - \mu(\lambda_{\mathrm{f}})m_3R_{\omega}\ddot{x}) \ , \\ \dot{\omega}_{\mathrm{r}} = \dfrac{1}{2J_{\mathrm{r}}}(-T_{\mathrm{br}} + \mu(\lambda_{\mathrm{r}})m_2R_{\omega}g + \mu(\lambda_{\mathrm{r}})m_3R_{\omega}\ddot{x}) \ . \end{cases} \tag{39}$$

Rewriting Eq. (39), then

$$\begin{cases} \dot{\omega}_{\mathrm{f}} = \dfrac{1}{2J_f}\mu(\lambda_{\mathrm{f}})(m_1R_{\omega}g - m_3R_{\omega}\ddot{x}) + \dfrac{-1}{2J_{\mathrm{f}}}T_{\mathrm{bf}} \ , \\ \dot{\omega}_{\mathrm{r}} = \dfrac{1}{2J_r}\mu(\lambda_{\mathrm{r}})(m_2R_{\omega}g + m_3R_{\omega}\ddot{x}) + \dfrac{-1}{2J_{\mathrm{r}}}T_{\mathrm{br}} \ . \end{cases} \tag{40}$$

Contained the term of the road friction coefficient of Eq. (40) were regarded as the perturbation of system, and for the expansion state variables of the system, we defined

$$\omega_{\mathrm{f}} = x_1, \ \frac{1}{2J_{\mathrm{f}}}\mu(\lambda_{\mathrm{f}})(m_1R_{\omega}g - m_3R_{\omega}\ddot{x}) = x_2, \ \omega_{\mathrm{r}} = x_3,$$
$$\frac{-1}{2J_{\mathrm{f}}} = b_1, \ \frac{1}{2J_{\mathrm{r}}}\mu(\lambda_{\mathrm{r}})(m_2R_{\omega}g + m_3R_{\omega}\ddot{x}) = x_4, \ \frac{-1}{2J_{\mathrm{r}}} = b_2,$$
$$T_{\mathrm{bf}} = u_1, \ T_{\mathrm{br}} = u_2.$$

Rewriting Eq. (40) into two integrator series system are, respectively, given by

$$\begin{cases} \dot{x}_1 = x_2 + b_1u_1 \ , \\ y_1 = x_1 \ . \end{cases} \tag{41}$$

$$\begin{cases} \dot{x}_3 = x_4 + b_2u_2, \\ y_2 = x_3 \ . \end{cases} \tag{42}$$

Using integrator series system of Eq. (41) as an example, second order linear extended state observer was designed as follows to observe the x_1 and x_2.

$$\begin{cases} e(k) = z_1(k) - y_1(k) \ , \beta_{01}{=}2\omega_0 \ , \quad \beta_{02}{=}\omega_0^2 \ , \\ z_1(k+1) = z_1(k) + h[z_2(k) - \beta_{01}e(k) + b_0u_1(k)], \\ z_2(k+1) = z_2(k) + h[-\beta_{02}e(k)], \end{cases} \tag{43}$$

where ω_0 is the bandwidth of linear extended state observer by pole assignment, u_1 and y_1 are the input signal, respectively, z_1 and z_2 are the output signal of linear extended state observer, which are the observations of the x_1 and x_2, b_0 is the estimation value of control gain b_1. From what has been discussed above, the observations of x_3 and x_4 can also be formulated as Eq. (42).

To estimate the road friction coefficient, substituting Eq. (40) into Eq. (41), a linear extended state observer was built as follows in detail:

$$\begin{cases} \omega_f = z_1, \\ \dfrac{1}{2J_{\mathrm{f}}}\mu(\lambda_{\mathrm{f}})(m_1R_{\omega}g - m_3R_{\omega}\ddot{x}) = z_2, \end{cases} \tag{44}$$

where z_1 and z_2 are the observations of the x_1 (front wheel angular speed) and x_2 (contain the term of the road friction coefficient). Likely,

$$\begin{cases} \omega_{\mathrm{r}} = z_3, \\ \dfrac{1}{2J_{\mathrm{r}}}\mu(\lambda_{\mathrm{r}})(m_2R_{\omega}g + m_3R_{\omega}\ddot{x}) = z_4, \end{cases} \tag{45}$$

where z_3 and z_4 are the observations of the x_3 (rear wheel speed) and x_4. Combining the Eqs. (44), (45), road friction coefficient of front and rear wheels can be formulated as

$$\begin{cases} \mu(\lambda_{\mathrm{f}}) = \dfrac{2J_{\mathrm{f}}z_2}{m_1R_{\omega}g - m_3R_{\omega}\ddot{x}}, \\ \mu(\lambda_{\mathrm{r}}) = \dfrac{2J_{\mathrm{r}}z_4}{m_2R_{\omega}g + m_3R_{\omega}\ddot{x}} \ . \end{cases} \tag{46}$$

If the estimation scheme of rear wheel is the same with front wheel, there is no need to show the estimation scheme of rear wheel.

5 Simulation Results

In this section, a number of simulations are carried out on the simulation software of ADAMS/Car simulating a vehicle in the virtual simulation environment to analyze and evaluate the estimation scheme proposed in this paper. While for road friction coefficient estimation, set vehicle model parameters in simulation as follows: $m = 1500$ kg, $m_{\mathrm{s}} = 1285$ kg, $m_{\mathrm{f}} = 96$ kg, $m_{\mathrm{r}} = 119$ kg, $l_{\mathrm{f}} = 1.186$ m, $l_{\mathrm{r}} = 1.258$ m, $h_{\mathrm{f}} = 0.3$ m, $h_{\mathrm{r}} = 0.3$ m, $R_{\omega} = 0.326$ m,

$J_f = 1.7$ kg m^2, $J_r = 1.7$ kg·m^2. The whole vehicle model in ADAMS/Car is shown in Fig. 3. A test environment for road with different friction coefficient was constructed using the compiler road builder in ADAMS/Car and the proposed road friction coefficient estimation method was tested in the constructed virtual environment.

The estimation method is constructed based on braking torque and wheel speed sensor. From what has been discussed above, the block diagram of road friction coefficient estimation scheme of front wheel is illustrated in Fig. 4.

5.1 High Friction Coefficient Road Surface

Ideal braking torque controller can make full use of road friction coefficient when vehicle braking. The braking torque of front and rear wheels is shown in Fig. 5 which is conducted on high friction coefficient of 0.8 and the initial longitudinal velocity of 30 m/s.

Fig. 6 shows the estimated road friction coefficient by second order linear extended state based on wheel speed and braking torque of front and rear wheels. As we can see from the figure, estimated road friction coefficient of front and rear wheels is very close to the real values of road friction coefficient. The largest difference between the estimated and the real values occurs about 0.3 s ago. It also can be seen that the front wheels of road friction coefficient estimation values is better than rear wheel. However, when vehicle braking, wheel speed signal has mixed with measurement noise and it assumed to be independent white Gaussian process with zero mean.

Fig. 7 shows the estimated road friction coefficient with noise interference. It is observed that the linear extended state observer estimated road friction coefficient with noise interference is also very close to the real values and exactly with strong robustness.

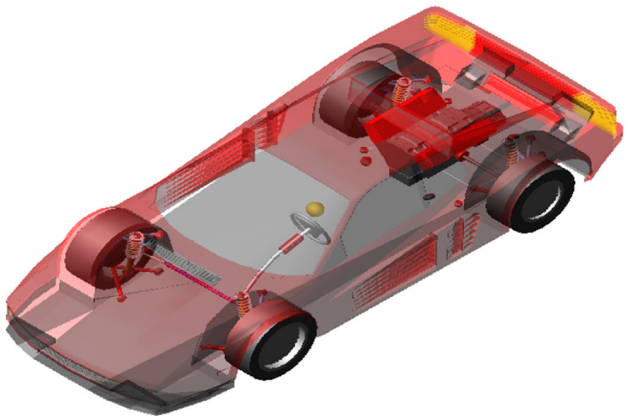

Fig. 3 Whole vehicle test model in ADAMS/Car

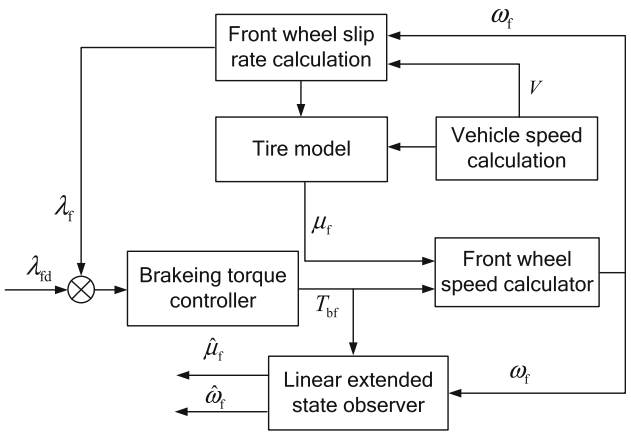

Fig. 4 Block diagram of road friction coefficient estimation scheme of front wheel

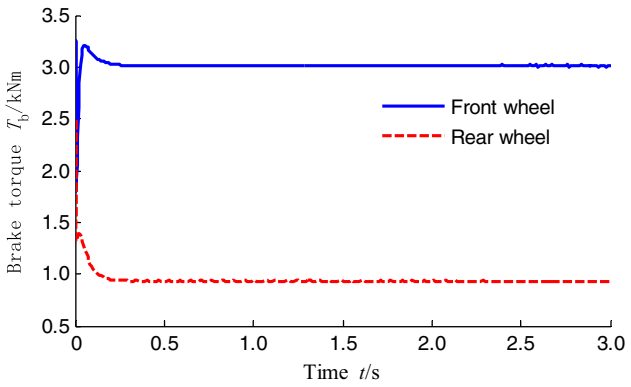

Fig. 5 Braking torque of front and rear wheels $\mu = 0.8$

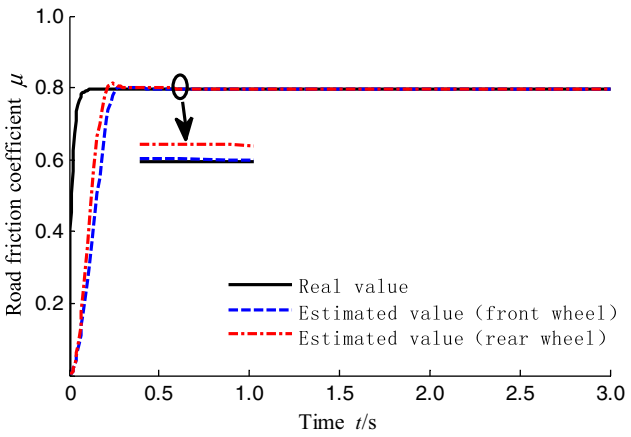

Fig. 6 Estimation of road friction coefficient $\mu = 0.8$

5.2 Low Friction Coefficient Road Surface

Fig. 8 shows the braking torque of front and rear wheels conducted on low friction coefficient of 0.2 and the initial longitudinal velocity of 30 m/s. The estimated values and real values of the road friction are presented in Fig. 9

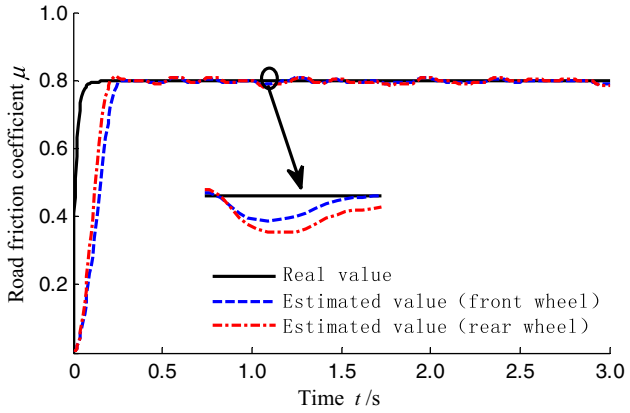

Fig. 7 Estimated road friction coefficient with noise interference $\mu = 0.8$

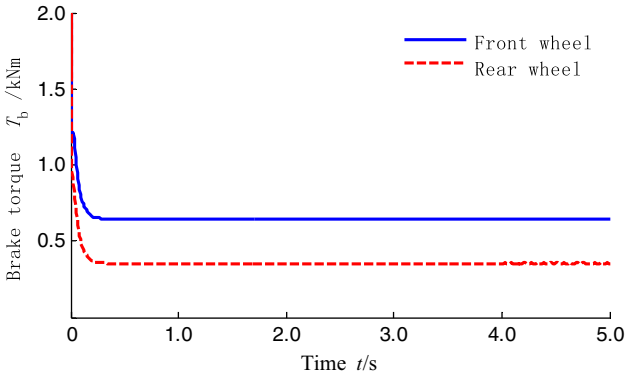

Fig. 8 Braking torque of front and rear wheels $\mu = 0.2$

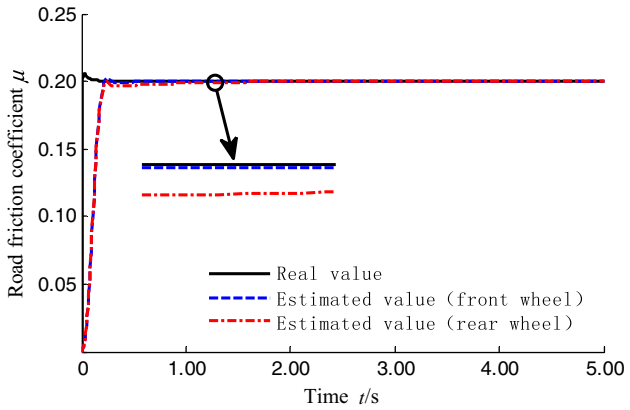

Fig. 9 Estimation of road friction coefficient $\mu = 0.2$

which indicates that the proposed estimator works well in low friction coefficient road surface and Fig. 10 shows the estimated road friction coefficient with noise interference respectively.

It can be easily seen that the proposed linear extended state observer can estimate the road friction coefficient, with good accuracy in comparison with the measurements

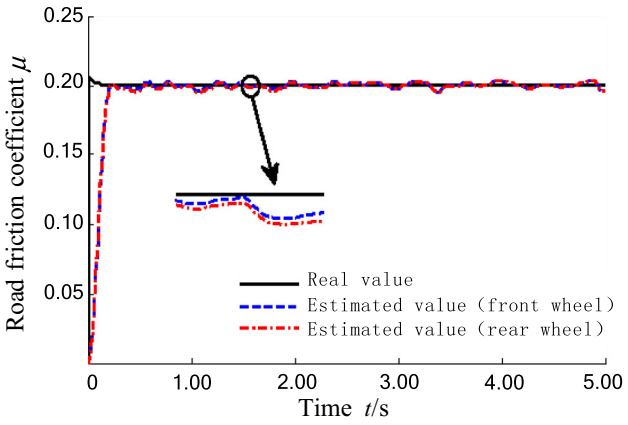

Fig. 10 Estimated road friction coefficient with noise interference $\mu = 0.2$

in vehicle braking on a single high or low friction coefficient road surface. Even in noise interference, it also can estimate road friction coefficient efficiently. However, the road friction coefficient estimation values of using the front wheels are better than rear wheels.

Next, simulations in uneven friction coefficient road conditions are discussed in detail.

5.3 Uneven Friction Coefficient Road

For road friction coefficient estimation in uneven friction road, the road surface with friction coefficients ranged from high to low and low to high are designed.

The braking torque of front and rear wheels is shown in Fig. 11(a) which is conducted on friction coefficients ranged from 0.8 to 0.2 and the initial longitudinal velocity of 30 m/s. Where, in 0 to 2 s, the vehicles are driven in high friction coefficient road surface and 2 to 7 s in the low friction coefficient road surface. Similarly, the braking torque of front and rear wheels conducted on friction coefficients ranged from 0.2 to 0.8 is shown in Fig. 11b. Where, in 0 to 2 s, the vehicles are driven in low friction coefficient road surface and 2 to 5 s in the high friction coefficient road surface. Respectively, the variations of estimated road friction coefficient in ideal condition are, with noise interference, given in Fig. 12.

We can easily find that the estimated road friction coefficient in ideal condition (Fig. 12(a), (c)) or measurement with noise interference (Fig. 12(b), (d)) is close to the reference values and the estimated values are less influenced by noise interference.

Though the road coefficients change greatly, the simulation results show that the proposed estimate method can still estimate road friction coefficient exactly with strong robustness, which can resist external disturbance.

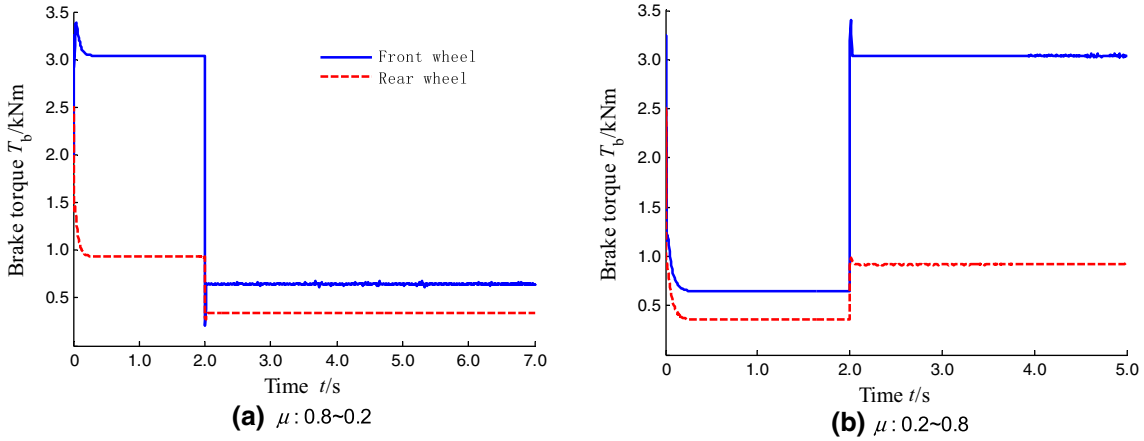

Fig. 11 Braking torque of front and rear wheels

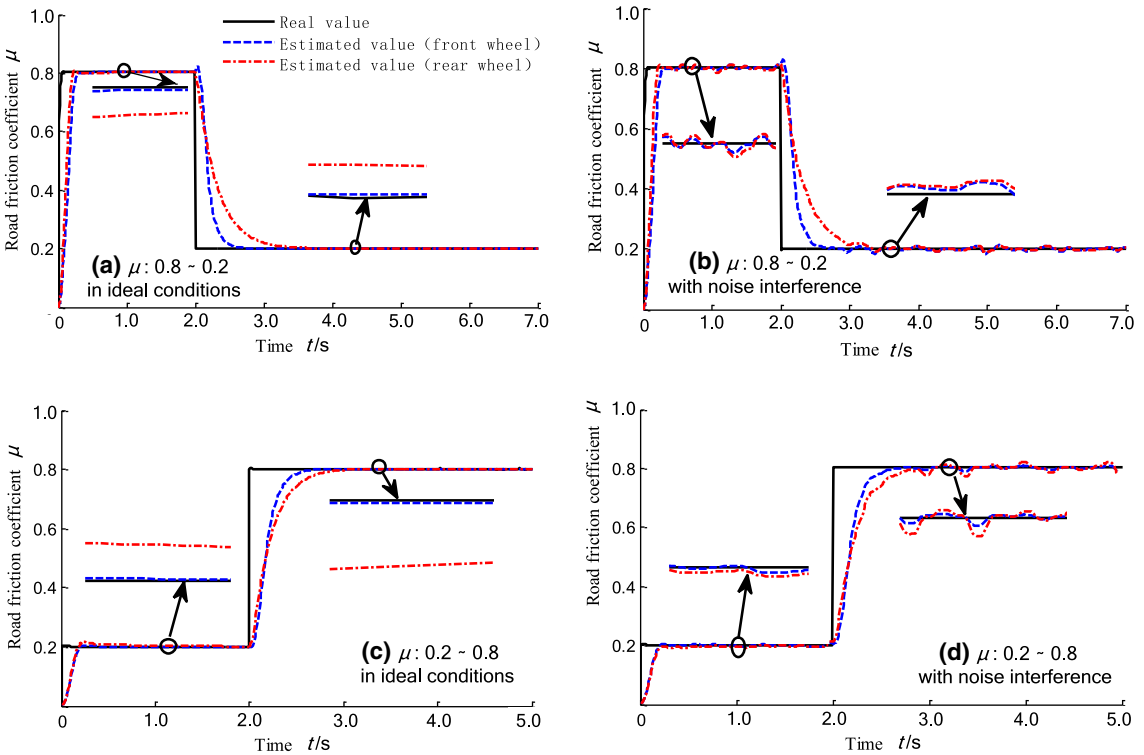

Fig. 12 Simulated and estimated road friction coefficient comparison

6 Conclusions

(1) According to the vehicle braking dynamics, the linear extended state observer to estimate the road friction coefficient is presented, which has a good accuracy when vehicle drive on the road of different friction coefficient.

(2) Using the method of saturation function and integral switching surface can eliminate chattering of sliding mode control.

(3) Simulation results using the front wheels of road friction coefficient estimation values are better than rear wheels.

(4) The proposed method has strong robustness in different road conditions, which can resist external disturbance.

References

1. R Isermann, R Mannale, K Schmitt. Collision-avoidance systems PRORETA: Situation analysis and intervention control. *Control Engineering Practice*, 2012, 20(11): 1236–1246.

2. J Wu, Y Q Zhao, X W Ji, et al. Generalized internal model robust control for active front steering intervention. *Chinese Journal of Mechanical Engineering*, 2015, 28(2): 285–293.
3. J Wu, Y H Liu, F B Wang, et al. Vehicle active steering control research based on two-DOF robust internal model control. *Chinese Journal of Mechanical Engineering*, 2016, 29(4): 1-8.
4. J Chen, J Song, L Li, et al. A novel pre-control method of vehicle dynamics stability based on critical stable velocity during transient steering maneuvering. *Chinese Journal of Mechanical Engineering*, 2016, 29(3): 475-485.
5. L Li, X Ran, K Wu, et al. A novel fuzzy logic correctional algorithm for traction control systems on uneven low-friction road conditions. *Vehicle System Dynamics*, 2015, 53(6): 711–733.
6. M Kang, L Li, H Li, et al. Coordinated vehicle traction control based on engine torque and brake pressure under complicated road conditions. *Vehicle System Dynamics*, 2012, 50(9): 1473–1494.
7. H Z Li, L Li, L He, et al. PID plus fuzzy logic method for torque control in traction control system. *International Journal of Automotive Technology*, 2012, 13(3): 441–450.
8. L LI, K Yang, G Jia, et al. Comprehensive tire–road friction coefficient estimation based on signal fusion method under complex maneuvering operations. *Mechanical Systems and Signal Processing*, 2015, 56(3): 259–276.
9. J Song, C Yang, H Z Li, et al. Road friction coefficient estimation based on multisensor data fusion for an AYC system. *Qinghua Daxue Xuebao/Journal of Tsinghua University*, 2009, 49(5): 715–718. (in Chinese)
10. G Li, R C Xie, S Y Wei, et al. Vehicle state and road friction coefficient estimation based on double cubature kalman filter. *Science China: Technological Sciences*, 2015, 45(4): 403–414. (in Chinese)
11. C Yang, L Li, J Song, et al. Road friction coefficient estimation algorithm based on tire force observer. *China Mechanical Engineering*, 2009, 20(7): 873–876. (in Chinese)
12. J O Hahn, R Rajamani, L Alexander. GPS-based real-time identification of tire-road friction coefficient. *IEEE Transactions on Control Systems Technology*, 2002, 10(3): 331–343.
13. G Erdogan, L Alexander, R Rajamani. Measurement of uncoupled lateral carcass deflections with a wireless piezoelectric sensor and estimation of tire road friction coefficient//*ASME 2010 Dynamic Systems and Control Conference*, Cambridge, Massachusetts, USA, Sep 12–15, 2010: 541–548.
14. G Erdogan, L Alexander, R Rajamani. Estimation of tire-road friction coefficient using a novel wireless piezoelectric tire sensor. *IEEE Sensors Journal*, 2011, 11(2): 267–279.
15. Z P Yu, J L Zuo, L J Zhang. A summary on the development status of tire-road friction coefficient estimation techniques. *Automotive Engineering*, 2006, 28(6): 546–549. (in Chinese)
16. K Enisz, I Szalay, G Kohlrusz, et al. Tyre-road friction coefficient estimation based on the discrete-time extended kalman filter. *Proceedings of the Institution of Mechanical Engineers, Part D: Journal of Automobile Engineering*, 2015, 229(9): 1158–1168.
17. K Enisz, D Fodor, I Szalay, et al. Improvement of active safety systems by the extended Kalman filter based estimation of tire-road friction coefficient//*2014 IEEE International Electric Vehicle Conference,* Florence, Italy, Dec 11-19, 2014: 1–5.
18. Y Q Zhao, F Lin. Estimation of road pavement adhesion factor based on virtual experiment. *Journal of Jilin University: Engineering and Technology Edition*, 2011, 41(2): 309–315. (in Chinese)
19. F Lin, C Huang. Unscented kalman filter for road friction coefficient estimation. *Journal of Harbin Institute of Technology*, 2013, 45(7): 115–120. (in Chinese)
20. T A Wenzel, K J Burnham, M V Blundell, et al. Dual extended kalman filter for vehicle state and parameter estimation. *Vehicle System Dynamics*, 2006, 44(2): 153–171.
21. F G Yang, Y B Li, J H Ruan, et al. Real-time estimation of tire road friction coefficient based on extended state observer. *Transactions of the Chinese Society for Agricultural Machinery*, 2010, 41(8): 6–9. (in Chinese)
22. L Ray. Nonlinear tire force estimation and road friction identification: simulation and experiments. *Automatica*, 1997, 33 (10): 1819–1833.
23. A Harifi, A Aghagolzadeh, G Alizadeh, et al. Designing a sliding mode controller for slip control of antilock brake systems. *Transportation Research Part C Emerging Technologies*, 2008, 16(6): 731–741.
24. M Bouri, D Thomasset. Sliding control of an electropneumatic actuator using an integral switching surface. *Control Systems Technology IEEE Transactions*, 2001, 9(2): 368–375.
25. Y Huang, J Q Han. Analysis and design for nonlinear continuous extended state observer. *Chinese Bulletin*, 2000, 45(21): 1938–1944.
26. Z Q Gao. Scaling and bandwidth-parameterization based controller tuning//*Proceedings of the 2003 American control conference*, Denver, Colrado, USA, Jun 4–6, 2003: 4989–4996.

You-Qun Zhao, born in 1968, is currently a professor in *Nanjing University of Aeronautics and Astronautics, China*. He received his PhD degree from *Jilin University, China*, in 1998. His research interests include vehicle system dynamics and mechanical elastic wheel. E-mail: yqzhao@nuaa.edu.cn

Hai-Qing Li, born in 1989, is currently a PhD candidate in *Nanjing University of Aeronautics and Astronautics, China*. He received his master degree on *Vehicle Engineering in Kunming University of Science and Technology, China*, in 2015. His research interests include vehicle dynamics control and autonomous vehicle control. E-mail: lito7989@163.com

Fen Lin, born in 1980, is currently an associate professor in *Nanjing University of Aeronautics and Astronautics, China.* He received his PhD degree from *Nanjing University of Aeronautics and Astronautics, China*, in 2008. His research interest is vehicle system dynamics. E-mail: flin_nuaa@163.com

Jian Wang, born in 1986, is currently work at *School of Automotive Engineering, Shandong Jiaotong University, China.* He received his PhD degree from *Nanjing University of Aeronautics and Astronautics, China*, in 2015. His research interests include vehicle active safety and automotive electronics. E-mail: wangjian1987228@163.com

Xue-Wu Ji, born in 1964, is currently a professor in *Tsinghua University, China*. He received his PhD degree from *Jilin University, China*, in 1994. His research interests include vehicle system dynamics and vehicle steering system. E-mail: jixw@tsinghua.edu.cn